Twelvefold Quasiperiodic Patterns in a Nonlinear Optical System with Continuous Rotational Symmetry

R. Herrero,* E. Große Westhoff, A. Aumann, T. Ackemann, Yu. A. Logvin,† and W. Lange
Institut für Angewandte Physik, Westfälische Wilhelms-Universität Münster, Corrensstraße 2/4, D-48149 Münster, Germany
(Received 19 October 1998)

Twelvefold quasiperiodic structures are observed in an autonomous optical pattern forming system with continuous rotational symmetry. These quasipatterns arise from a primary hexagonal structure. In dependence on the experimental parameters the bifurcation can be sub- or supercritical. In the supercritical case, the transition is mediated by a new kind of patterns with different amplitudes in its fundamental modes. It is proven by an optical Fourier filtering technique that the observed quasipatterns can exist only in the presence of harmonics of the fundamental unstable modes. [S0031-9007(99)09326-6]

PACS numbers: 42.65.Sf, 42.60.Jf, 47.54.+r

Periodic planar patterns have a translational symmetry and an N-fold discrete rotational symmetry with $N = 2$, 3, 4, or 6. The typical structures, stripes, rhombi, squares, and hexagons, have been investigated in dissipative systems for several years [1]. N-fold rotational symmetries with $N = 5$ or $N > 6$ are incompatible with translational symmetry. Therefore the corresponding structures are not periodic, but quasiperiodic [2]. These quasipatterns have been predicted to occur in a large variety of dissipative systems with initial $O(2)$ symmetry [3–6]. Their general properties have been the subject of considerable theoretical interest [7–12].

Experimental evidence, however, has been limited to the Faraday experiment, i.e., to a parametrically excited hydrodynamical system [13–15]. In these experiments eight- and tenfold quasiperiodic patterns have been obtained in a situation characterized by inversion symmetry (with respect to the order parameter). In the more general case of broken inversion symmetry, dodecagonal quasipatterns ($N = 12$) are expected in many systems [5–8,10]. In the Faraday system, however, their observation has been restricted to a fairly special situation, close to a codimension-two point. Furthermore, quasipatterns have been observed in optical systems upon which a discrete rotational symmetry was imposed externally [16].

In this paper, we report the experimental observation and numerical simulation of stationary twelvefold quasiperiodic patterns in an optical system with continuous rotational symmetry. In a large parameter range these quasipatterns arise via a secondary bifurcation from a primary hexagonal structure. Moreover, we report on a new type of quasipatterns which might be interpreted as a mixed state between hexagons and twelvefold quasipatterns. In our studies, we make use of a genuine advantage of optical pattern forming systems, i.e., the real time access to the Fourier transform of the pattern which can be used in a Fourier filtering technique [6]. In this way it is proven *experimentally* that in the system under study spatial harmonics of the fundamental Fourier modes are essential in the stabilization of the quasipatterns.

The experimental system (cf. Fig. 1) is built from a nonlinear medium and a single mirror [17,18]. The nonlinear medium is sodium vapor in a buffer gas atmosphere (nitrogen at a pressure p_{N_2} of 200–300 hPa) which is contained in a heated cell (length $L = 15$ mm) (cf. also [19]). A cell temperature $T \approx 300\,^\circ\mathrm{C}$ results in a particle density of $N \approx 2 \times 10^{19}\ \mathrm{m}^{-3}$. The medium is irradiated by the carefully spatially cleaned Gaussian output beam of a dye laser which is tuned to a frequency slightly above the frequency of the sodium D_1 line (frequency detuning $\Delta = \nu_{\mathrm{laser}} - \nu_{D_1}$). The light is circularly polarized and represents σ_+ light with respect to the quantization axis defined by a weak longitudinal magnetic field. (The transverse component of the magnetic field is smaller than 1 μT.) The beam waist (radius $w_0 = 1.5$ mm) lies in the center of the sodium cell. The transmitted light is fed back into the medium by a single plane mirror (reflectivity $R = 0.915$), placed at a distance d of about 80 to 150 mm behind the medium. The near and far field intensity distributions of the forward beam transmitted by the mirror are imaged onto two CCD cameras. The essential modification with respect to the setup used before [19] is the insertion of a quarter-wave plate in the feedback loop which transforms the σ_+ polarization of the forward beam into a σ_- polarization of the feedback beam [20] (see also [21]).

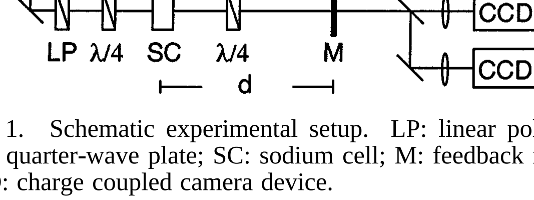

FIG. 1. Schematic experimental setup. LP: linear polarizer; $\lambda/4$: quarter-wave plate; SC: sodium cell; M: feedback mirror; CCD: charge coupled camera device.

When the input power is increased from zero, a first bifurcation from the homogeneous state to hexagonal structures occurs. In the near field, structures of the type shown in Fig. 2a are observed, while we obtain the distribution of Fig. 2b in the far field. The six spots result from the presence of six transverse wave vectors mutually at an angle of $\pi/3$. This configuration of three pairs of wave vectors is usually referred to as the hexagonal triad. The strong confinement of the maxima of the far field intensity distribution indicates that the description of the patterns in terms of Fourier modes is appropriate and that the pattern forming process should not significantly be affected by the finite size of the Gaussian beam.

For increasing input power, we observe a secondary bifurcation to a different type of stationary structure. In the near field these structures are of the type displayed in Fig. 2c; i.e., they are no longer periodic and appear to be rather irregular. In the far field, however, the structures are regular (Fig. 2d). They consist of twelve intense maxima of alternating intensity evenly distributed on a circle. These patterns can be thought of as being formed by two triads of wave vectors which are rotated with respect to each other by an angle of $\pi/6$ (cf. Fig. 3a).

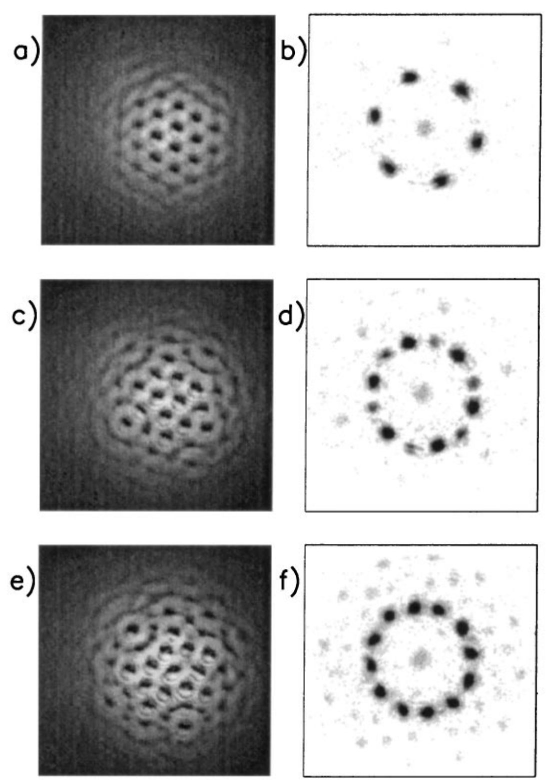

FIG. 2. Experimentally observed near [(a),(c),(e)] and far field [(b),(d),(f)] images of the transmitted beam. The contrast of the far field images has been digitally enhanced. Parameters: $p_{N_2} = 200$ hPa, $T = 300\,^\circ$C, $\Delta = +4$ GHz, $d = 91$ mm. The input power is 78 mW in (a),(b), 88 mW in (c),(d), and 100 mW in (e),(f). The frame size of the near field images is 3×3 mm^2.

A further increase of the input power yields patterns in which the power in the two triads is equal (cf. Figs. 2e and 2f). This configuration of wave vectors is known to form a twelvefold quasiperiodic pattern in real space (see, e.g., [8]). Keeping all parameters constant, we observe different near field patterns for the same far field intensity distribution. Therefore, we interpret these patterns as different parts of a spatially extended quasipattern.

For a closer examination of the bifurcation scenario, we determined the dependence of the power in the two triads on the input power (cf. Fig. 4). While the power in the first triad remains approximately constant, the power in the second triad grows steadily from very low values at the threshold of the secondary bifurcation until the power of the primary triad is reached far above threshold.

The behavior just described indicates that we encounter a supercritical bifurcation from hexagons to twelvefold quasipatterns that is mediated by a new type of patterns. We are not aware of any observation or prediction of patterns composed of two triads with different amplitudes. These patterns are quasiperiodic, since they can be thought of as the superposition of a (hexagonal) periodic and a (twelvefold) quasiperiodic structure. They might be interpreted as stable mixed states between hexagons and twelvefold quasipatterns.

The supercritical bifurcation is typical for small frequency detunings, while for larger detunings, we observe a direct transition from the hexagonal to the twelvefold quasiperiodic structures. The transition is accompanied by bistability. These observations indicate that the bifurcation is subcritical far from resonance.

Let us now turn to a more quantitative analysis of a typical quasipattern, as displayed in Fig. 2f. In addition to the fundamental Fourier modes with the wave number q_0, we observe further sets of (weak) Fourier modes with twelvefold rotational symmetry at higher spatial frequencies. The wave numbers of the most intense ones are $1.43q_0$, $1.64q_0$, and $1.95q_0$. These values were obtained from averaging the length of corresponding wave vectors and have a standard deviation of about $0.1q_0$. They agree reasonably well with the values $q_1 = 2\cos(\frac{\pi}{4})q_0 \approx 1.41q_0$, $q_2 = 2\cos(\frac{\pi}{6})q_0 \approx 1.73q_0$, and $q_3 = 2\cos(\frac{\pi}{12})q_0 \approx 1.93q_0$, respectively, which are obtained from the addition

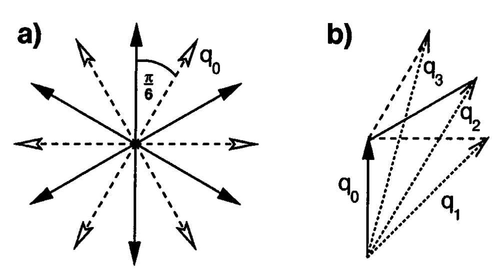

FIG. 3. (a) Superposition of two hexagonal triads (solid and broken arrows); (b) generation of spatial harmonics via addition of fundamental wave vectors.

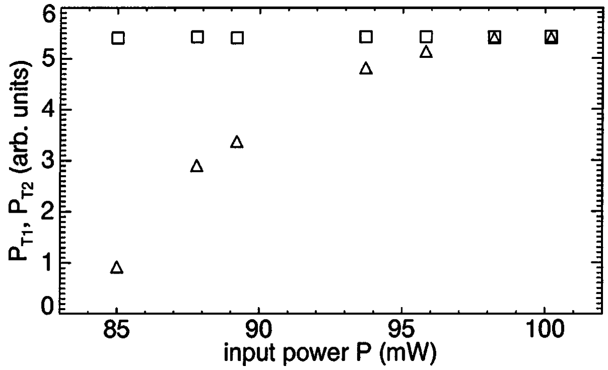

FIG. 4. Power in the primary (P_{T1}, denoted by squares) and secondary (P_{T2}, denoted by triangles) triads of Fourier modes. Parameters as in Fig. 2.

of two fundamental wave vectors (cf. Fig. 3b). This addition of two wave vectors to form a third one ("3-wave mixing") is typical for nonlinear systems with quadratic interactions.

It has been argued that a quadratic interaction of harmonic Fourier modes with fundamental modes can be essential in stabilizing twelvefold structures [7,8,10]. In order to examine the role of the harmonics experimentally, we insert a low-pass Fourier filter in the feedback loop [6]. The filter consists of a confocal telescope with an iris aperture in the focal plane where the Fourier transform is available. The focal length of both lenses is $f = 150$ mm. The first lens is located at a distance f from the sodium cell. The feedback mirror is placed at a distance $f + d$ behind the second lens and acts as a "virtual" mirror [22] located at a distance d from the cell. No qualitative change with respect to the results without the telescope has been found in the observed structures as long as the aperture is open.

When the aperture radius is decreased, the quasipatterns give way to hexagons, which may have a slightly different fundamental wave number. As an example, the far field of a quasiperiodic structure obtained for an open aperture is shown in Fig. 5a. Keeping all the other parameters

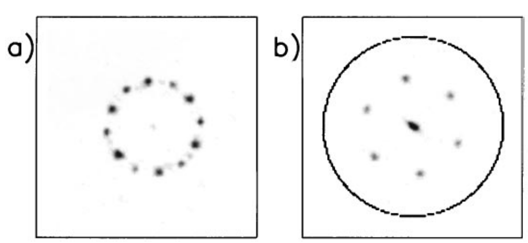

FIG. 5. Far field patterns observed with a Fourier filter in the feedback loop. The aperture is open in (a); in (b) it corresponds to a maximum transverse wave vector of $q_{\max} = 35.1\ \mathrm{mm}^{-1}$, which is indicated by the black circle. The fundamental wave number of the quasipattern in (a) is $q_0 = 18.5\ \mathrm{mm}^{-1}$, the fundamental wave number of the hexagonal pattern is $q_0' = 19.1\ \mathrm{mm}^{-1}$. Parameters: $p_{\mathrm{N}_2} = 300$ hPa, $T = 297\,^\circ$C, $\Delta = +4$ GHz, $d = 150$ mm, input power 140 mW.

constant, we decrease the diameter of the aperture. The quasipattern remains stable down to an aperture size corresponding to a cutoff wave number of $q_{\max} = 1.9 q_0$ (cf. Fig. 5), where q_0 is the fundamental wave number of the quasipattern for an open aperture. For an aperture size below a threshold value, the quasipattern is replaced by a hexagonal pattern. Within the margins of error the cutoff frequency agrees with the spatial frequency of the harmonics at $q_3 \approx 1.93 q_0$.

In the theoretical description of our system, we follow the approach described in [18]. In contrast to the Kerr medium assumed in [18] sodium vapor is saturable. The spin of the atoms brings pronounced tensor properties of the nonlinearity into play. Under the conditions of our experiment the sodium D_1 line can approximately be modeled as a homogeneously broadened $J = \frac{1}{2} \leftrightarrow J' = \frac{1}{2}$ transition with a negligible population of the excited state [23]. An intensity difference between the circular polarization components (pump rates $P_\pm$) of the light field creates a population difference w between the Zeeman sublevels of the ground state, which decays very slow ($\gamma \approx 1.5\ \mathrm{s}^{-1}$). w determines the susceptibility of the medium [23]. The medium is considered to be thin, so that diffraction within it can safely be neglected. However, because of the opposite circular polarization of the forward and backward beams, absorption is rather strong and the resulting pump depletion has to be accounted for. Following the approach developed in [24], we derive an equation of motion for the mean orientation $\Phi(x,y) = \frac{1}{L}\int_0^L w(x,y,z)\,dz$, averaged over the length L of the medium (cf. Ref. [20] for details):

$$\frac{\partial}{\partial t}\phi = -(\gamma + D\nabla_\perp^2)\phi + \frac{1}{2L\alpha_0}\left(1 - e^{-2L\alpha_0(1-\phi)}\right)P_+^f(0) - \frac{1}{2L\alpha_0}\left(1 - e^{-2L\alpha_0(1+\phi)}\right)P_-^b(L).$$

D is the atomic diffusion coefficient and $2\alpha_0$ is the linear absorption coefficient. The σ_--polarized field $E_-^b(L)$ reentering the sodium cell is derived from the σ_+-polarized input field $E_+^f(0)$ by

$$E_-^b(L) = R e^{-i(d/k_0)\nabla_\perp^2} e^{-L\alpha_0(1-i\bar{\Delta})(1-\phi)} E_+^f(0).$$

Here R is the reflectivity of the mirror and the spatial operator $\exp(-i\frac{d}{k_0}\nabla_\perp^2)$ describes the diffraction of the forward and the backward beams in the free space between cell and mirror. k_0 is the wave number of the light and $\bar{\Delta} = 2\pi\Delta/\Gamma_2$ is determined by the detuning and the relaxation rate of the optical coherences Γ_2.

Assuming a plane wave input, we investigate the linear stability of the homogeneous state with respect to sinusoidal perturbations. The marginal instability curve shows the typical structure for the single feedback mirror arrangement which is a sequence of instability balloons [18]. For

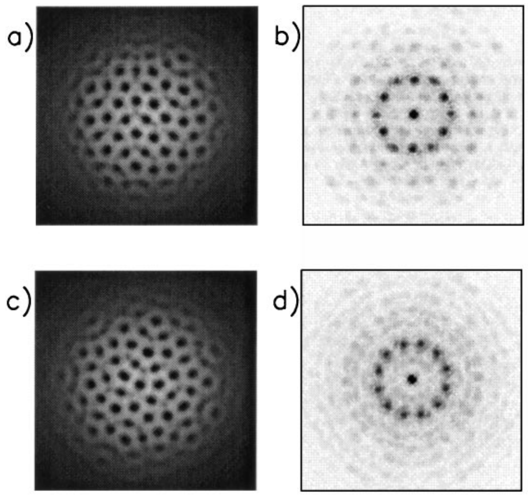

FIG. 6. Numerical simulation of a quasiperiodic structure for a buffer gas pressure 300 hPa, cell temperature 307 °C, the detuning 6 GHz, mirror distance $d = 81$ mm, beam waist $w_0 = 1.5$ mm, input power 145 mW for (a),(b) and 150 mW for (c),(d). The frame size of the near field [(a),(c)] images is 4×4 mm^2; the corresponding contrast enhanced far field distributions are shown in (b),(d).

increasing input power the instability balloons successively become unstable in the order of the wave numbers they contain.

The linear stability analysis qualitatively reproduces the frequency dependence of the observed threshold for the first bifurcation. There is also a good agreement between the fundamental wave number q_0 in the experiment and the minimum of the first instability balloon [20]. This correspondence is a further indication that the spatial variation of the stress parameter given by the Gaussian beam has a negligible impact on the pattern formation process.

There is a near coincidence between the harmonics q_3 and the minimum of the third instability balloon. It has been emphasized that the existence of the higher instability balloons in optical systems favors the formation of quasipatterns [5,6,25]. In the parameter range displaying quasipatterns in the experiment and in numerical simulations (see below) all higher harmonics are passive. This fact suggests that the mechanism of quadratic coupling proposed in Ref. [6,7,10] is of importance for the stabilization of quasipatterns even if it is provided by (weakly damped) passive modes (cf. also [12] and [25]).

Numerical simulations reproduce the appearance of negative hexagons at threshold and the supercritical secondary bifurcation to twelvefold quasipatterns (cf. Fig. 6). The subcritical bifurcation has not been reproduced yet. It should be noted, however, that in Fig. 6b the wave numbers in the two triads are slightly different. As in the experiment, the quasipatterns give way to hexagons, if the harmonics at q_3 are suppressed by a filter in Fourier space. Moreover, the simulations reveal that also the removal of the harmonics at q_1 or the ones at q_2 suppresses the quasipatterns. Thus it is evident from both the experiment and the simulation that harmonics of the fundamental Fourier modes are crucial in the formation of the quasipatterns.

*Permanent address: Department de Fisica, Campus Edifici Cc, Universitat Autonoma de Barcelona, Es-08193 Bellaterra (Barcelona), Spain.
†Permanent address: Institute of Physics, Belarus Academy of Sciences, Minsk 220072, Belarus.

[1] M. C. Cross and P. Hohenberg, Rev. Mod. Phys. **65**, 851 (1993).
[2] C. Janot, *Quasicrystals: a Primer* (Oxford University Press, New York, 1994), 2nd ed.
[3] F. J. Elmer, Phys. Rev. Lett. **70**, 2028 (1993).
[4] A. A. Golovin, A. A. Nepomnyashchy, and L. M. Pismen, Physica (Amsterdam) **81D**, 117 (1995).
[5] D. Leduc, M. Le Berre, E. Ressayre, and A. Tallet, Phys. Rev. A **53**, 1072 (1996).
[6] E. V. Degtiarev and M. A. Vorontsov, J. Mod. Opt. **43**, 93 (1996).
[7] N. D. Mermin and S. M. Troian, Phys. Rev. Lett. **54**, 1524 (1985).
[8] B. A. Malomed, A. A. Nepomnyashchii, and M. I. Tribel'skii, Sov. Phys. JETP **69**, 388 (1989).
[9] A. C. Newell and Y. Pomeau, J. Phys. A **26**, L429 (1993).
[10] H. W. Müller, Phys. Rev. E **49**, 1273 (1994).
[11] R. Lifshitz and D. M. Petrich, Phys. Rev. Lett. **79**, 1261 (1997).
[12] P. Chen and J. Viñals, Phys. Rev. Lett. **79**, 2670 (1997).
[13] B. Christiansen, P. Alstrøm, and M. T. Levinsen, Phys. Rev. Lett. **68**, 2157 (1992).
[14] W. S. Edwards and S. Fauve, Phys. Rev. E **47**, R788 (1993).
[15] D. Binks and W. van de Water, Phys. Rev. Lett. **78**, 4043 (1997).
[16] E. Pampaloni, P. L. Ramazza, S. Residori, and F. T. Arecchi, Phys. Rev. Lett. **74**, 258 (1995).
[17] G. Giusfredi, J. F. Valley, R. Pon, G. Khitrova, and H. M. Gibbs, J. Opt. Soc. Am. B **5**, 1181 (1988).
[18] G. D'Alessandro and W. J. Firth, Phys. Rev. Lett. **66**, 2597 (1991); G. D'Alessandro and W. J. Firth, Phys. Rev. A **46**, 537 (1992).
[19] T. Ackemann, Yu. A. Logvin, A. Heuer, and W. Lange, Phys. Rev. Lett. **75**, 3450 (1995).
[20] A. Aumann, E. Große Westhoff, R. Herrero, T. Ackemann, and W. Lange, J. Opt. B **1**, 166 (1999).
[21] A. J. Scroggie and W. J. Firth, Phys. Rev. A **53**, 2752 (1996).
[22] M. Tamburrini, E. Ciaramella, and E. Santamato, Chaos Solitons Fractals **4**, 1355 (1994).
[23] F. Mitschke, R. Deserno, W. Lange, and J. Mlynek, Phys. Rev. A **33**, 3219 (1986).
[24] M. Le Berre, D. Leduc, E. Ressayre, A. Tallet, and A. Maître, Opt. Commun. **118**, 447 (1995).
[25] M. Le Berre, D. Leduc, E. Ressayre, and A. Tallet, Asian J. Phys. **7**, 483 (1998) (special issue on *Nonlinear Dynamics in Optics*).